Journal Homepage: -www.journalijar.com

INTERNATIONAL JOURNAL OF ADVANCED RESEARCH (IJAR)

ISSN NO. 2320-5407

Article DOI:10.21474/IJAR01/15010
DOI URL: http://dx.doi.org/10.21474/IJAR01/15010

RESEARCH ARTICLE

DYNAMICAL EFFECTS OF A HOT DISK ON THE DEVELOPMENT OF A NATURAL CONVECTION FLOW BETWEEN CYLINDRICAL WALLS

Z. Yahya and Nouf Abdulaziz Alharbi
Department Of Physics, College Of Science, Qassim University, Buraidah, Saudi Arabia.

Manuscript Info

Manuscript History
Received: 05 May 2022
Final Accepted: 08 June 2022
Published: July 2022

Key words:-
CFD Algorithm, Numerical Modeling, Simpler, Navier-Stokes Equations. Source Position, Thermosiphon

Abstract

This study numerically investigates the problem of natural convection flow ina vertical cylinder. The importance of this issue mainly stems from thermal systems (e.g. chimneys, hot air generators, solar collectors, and many others.). Despite the numerous studies on the modeling of free convection flow between two perpendicular plates, there are very few studies that have investigated regarding the convective flow between two cylindrical walls. Therefore, the study is limited to vertical cylinders with different heating modes.The first configuration includes heated walls of thermosiphon flow in a cylindrical channel.The second configuration introduces a circular heat source at the channel entrance, and the third configuration includes an ended vertical cylinder with a heat source centered in the cylinder (zs = 0.04). The flow comparison from the three configurations demonstrates how the hot disk affects the flow from a dynamic point of view.Furthermore, details about the flow and dynamical fields can be obtained from the solution equation of the conservation of momentum and energy, considering the differences between the boundary conditions of the studied configurations. The study covers Rayleigh numbers and focuses on the effect of the cylinder's geometry on the characteristic of the flow as well as dynamical and thermal field characteristics and variations in Nusselt number. The studied flow is natural convection, laminar, steady, two-dimensional, and incompressible flow. Solutions were obtained using a numerical model based on the finite volume method and the Navier–Stokes equations. The velocity–pressure coupling was resolved using the SIMPLER algorithm. The temperature and vertical velocity profiles of the flow showed the existence of a boundary layer regime along the heated channel wall without a heat source. The layer continued along the cylindrical wall with the introduction of the heat source at the channel inlet. However, introducing the heat source caused a considerable change in the flow structure at the channel's central part.Calculations were performed for the channel aspect ratio R* = 0.2 and different Rayleigh numbers (Ra = 10^5, 10^7, 10^8, 10^9 and 10^{10}). Numerical results included velocity, temperature, and Nusselt number profiles.

Corresponding Author:- Z. Yahya
Address:- Department Of Physics, College Of Science, Qassim University, Buraidah, Saudi Arabia.

Introduction:-

Industrial chimney emissions are among the principal causes of air pollution that are difficult to control, making it necessary to study this type of pollutant and find solutions to reduce its impact on the environment. In this context, the numerical modeling of polluting emissions is considered an effective tool to identify such emissions and their dispersion as well as the physical variables of the polluting flow such as velocity and temperature, which can contribute to the proposition of preventive solutions to control air pollution.

The natural convection study in a hot cylindrical channel is a situation frequently encountered in many thermal systems such as chimneys, hot air generators, solar collectors, and ventilation of buildings.

In the beginning, the experiment proves the advantages of the confinement channels studied by Naffouti et al. [1] to investigate the characteristic of the free thermal plume introduced by the hot source and then surround it with two walls. They found increases in the flow rate, which helps to reach the flattened velocity profile at the exit of the channel. The other studies are interestedin geometry and its influence on fluid flow. Terekhov and Ekaid [2], studied numerically the behavior of the steady laminar flow inside the vertical channel for constant wall temperature and investigate the relation of the length and the width of the channel on the flow at a very large range Ar=1~200. They found that the effect of the aspect ratio on the flow temperature inside the channel increases with the increase of the aspect ratio and Nusselt number decreases. Because of the buoyancy force, the Reynold number increased when the Rayleigh number and aspect ratio increased.

Kettleborough [3] has studied numerically the laminar two-dimensional natural convection of fluid in a heated open-ended channel. He found that at higher values of Grashof number the buoyancy forces are very strong which increases the velocity of the fluid. In addition, the increase of Grashof number gives an increase in the Nusselt number and the maximum velocity at the exit. The transition between flow regimes depends on the particle volume fraction and Reynolds number in the channel was studied by Lashgari et al. [4] and the authors found that the critical value of Reynolds number is found to be $\mathrm{Re} \approx 2300$.

The structure of the flow of natural convection generated by a hot source placed at the entrance of an open vertical cylinder was studied experimentally by Mahmoud [5], the author has shown that the vertical evolution of the flow can be divided into three zones. A first zone is characterized by the formation of rotating rolls above the hot source, a second zone of the turbulence transition, and a third zone where the flow becomes established in the upper part of the cylinder, which is agreed with the paper [6]. While the free thermal plume has two discrete zones, the plume development, and established turbulence zones [1].

Zinoubi et al. [7]show that the optimal position of the hot source is located at h=-5cm from the entrance whereas the flow at the exit will be more homogenous than in other locations because the increasing of the source-cylinder spacing causes an entrance for the air creating a structure like the free plume. Taking these advantages and the adequate location for the industrial chimney will improve the dispersion of the air pollution reach.

This theoretical and numerical study seeks to improve knowledge of the dynamical effects of a hot disk on the development of a natural convection flow in a vertical cylinder. The studied model is based on the finite volume method to solve the Navier-Stokes equations for boundary conditions relating to the cylindrical channel. The velocity-pressure coupling was resolved using the SIMPLE algorithm. Results were obtained using Fortran code.

Pre-processing (Mathematical Formulation)

In this work we use the computational fluid dynamic (CFD) analysis to simulate the studied problem. This process contains three main steps as shown in Fig.1.

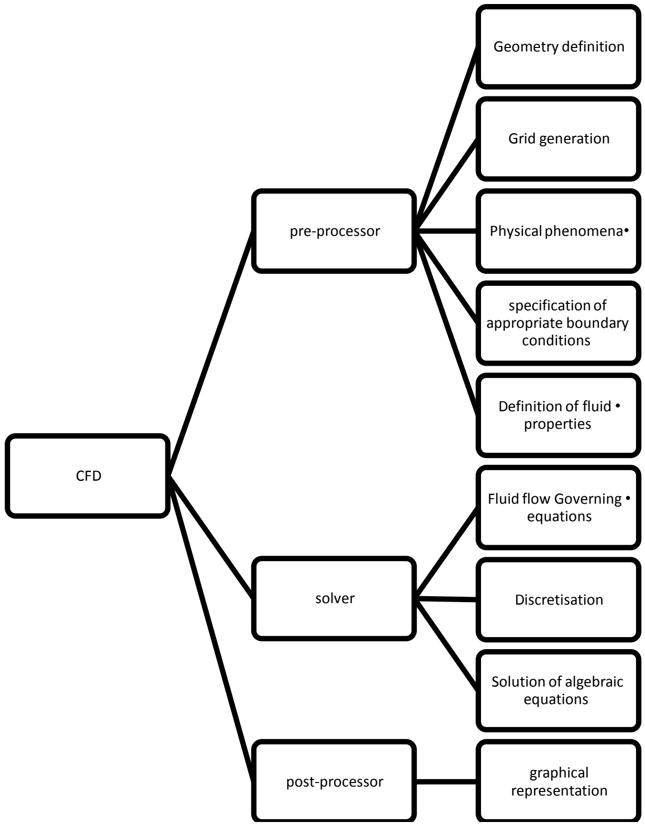

Figure 1:- CFD Analysis Process.

I-1 Geometry and boundary conditions

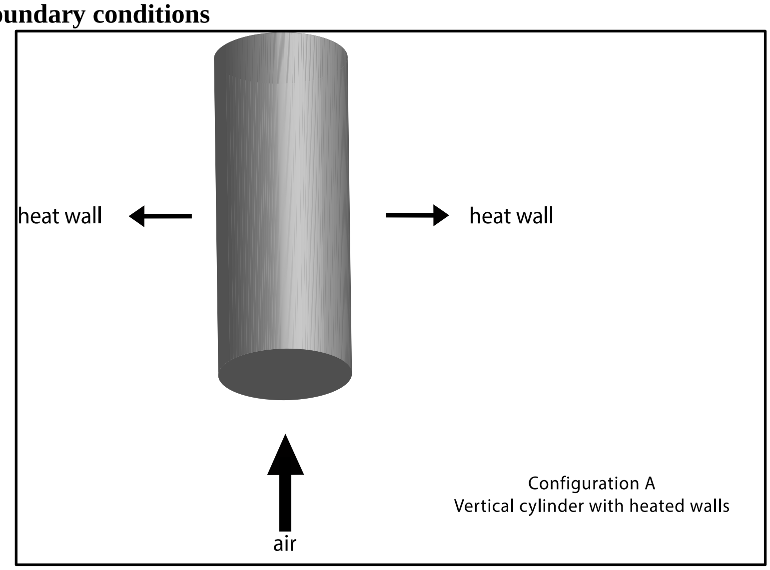

Figure 2:- Vertical channel with heated walls.

The first configuration is with boundary conditions of the thermosiphon flow in a cylindrical channel

At the wall

at $r = R;\ V_r = V_z = \frac{\partial P}{\partial z} = 0$

$T^* = \frac{(T_w - T_0)}{(T_s - T_0)}$ (1)

Along the axis of symmetry (r = 0), the boundary conditions are:

$\frac{\partial V_r}{\partial r} = \frac{\partial V_z}{\partial r} = \frac{\partial T^*}{\partial r} = 0$(2)

Inlet Condition

at$Z = 0\ \ V_r = \frac{\partial V_z}{\partial z} = 0;\ P = -\frac{1}{2}V_m^2$ (3)

V_m is the dimensionless average speed at the entry

$T^* = 0$

Outlet Condition

at $z = 1$

$\frac{\partial v_r}{\partial z} = \frac{\partial v_z}{\partial z} = \frac{\partial p}{\partial z} = 0$ (4)

$\frac{\partial T^*}{\partial z} = 0$ (5)

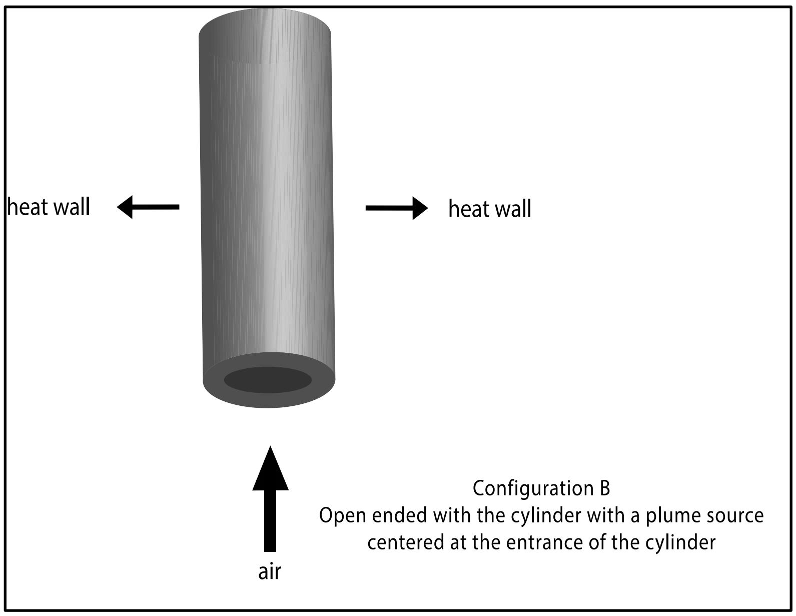

Figure 3:- Open-ended vertical cylinder with a plume source centered at the cylinder inlet.

The second configuration introduces a circular heat source at the channel inlet withadifferent radius of the circular hot disk (R*=0.2). With the flow of Rayleigh number Ra = 10^7, the boundary conditions arethesame in configuration A except for the inlet with a heating source (hot disk).

At z = zs

$0 \leq r \leq R_s\ , V_z = V_r = P = 0\ , T^* = 1$ (6)

The third configuration is an ended vertical cylinder with a heat source centered in the cylinder (zs = 0.04). The boundary conditions are the same in configuration A expect the symmetry axis with a heating source (hot disk). Along the symmetry axis (r = 0), the boundary conditions are

$\frac{\partial v_r}{\partial r} = \frac{\partial v_z}{\partial r} = 0 T^* = 1$(7)

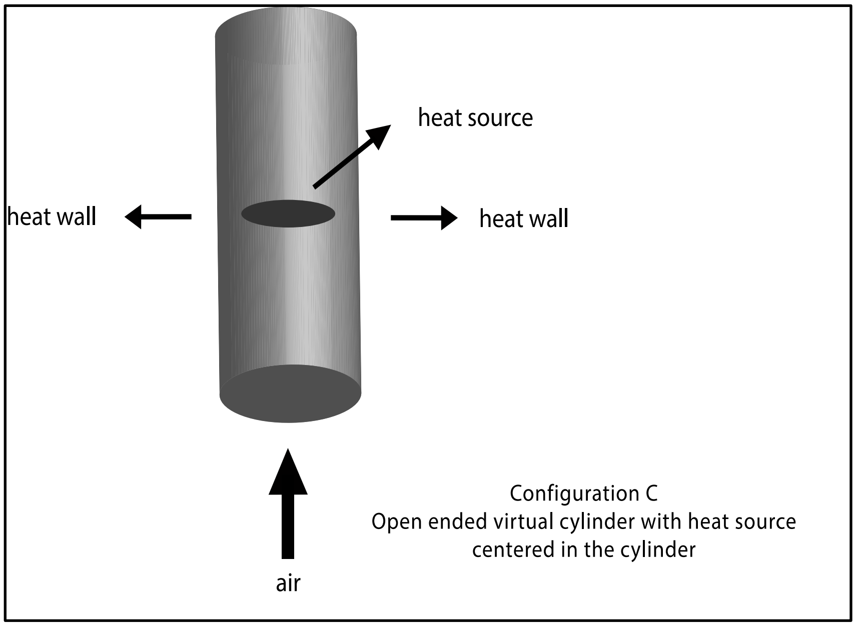

Figure 4:- Open-ended vertical cylinder with a heat source centered in the cylinder (zs = 0.04).

I-2 Fluid proprieties and physical phenomena

The flow is natural convection flow, supposed as:

1. laminar, which means the fluid flow moves smoothly or in regular paths (no fluctuations in velocity, pressure, temperature)
2. steady (time-independent)
3. symmetric to the cylinder's axis, the cylindrical polar coordinate system is chosen to describe the geometry and semi-vertical r–z plane (Axisymmetric $\frac{\partial}{\partial\theta} = 0$.)
4. two dimensional.

The fluid is a Newtonian, viscous, transparent and incompressible
(ρ is constant; $\frac{\partial\rho}{\partial t} = 0$). The physical proprieties are constant except for the density in the motion equation.

Solver (Numerical Modelling)

The second step of the CFD (Figure 1).

II-1 General Governing Equation

The dimensionless equations that govern the heat transfers in the three configurations

$$\mathrm{div}\vec{V} = 0 \quad (8)$$

$$\mathrm{div}\left[\vec{V}V_r - \mathrm{Pr}\,\mathrm{Ra}^{-\frac{1}{2}}\overrightarrow{\mathrm{grad}}V_r\right] = -\frac{\partial P^*}{\partial r^*} - \mathrm{Pr}\,\mathrm{Ra}^{-\frac{1}{2}}\frac{V_r}{r^{*2}} \quad (9)$$

$$\mathrm{div}\left[\vec{V}V_z - \mathrm{Pr}\,\mathrm{Ra}^{-\frac{1}{2}}\overrightarrow{\mathrm{grad}}V_z\right] = -\frac{\partial P^*}{\partial Z^*} - \mathrm{Pr}.\,T^* \quad (10)$$

$$\mathrm{div}\left[\vec{V}T^* - \mathrm{Ra}^{-\frac{1}{2}}\mathrm{g}\right.$$

II-2 The finite volume method

The finite volume method(FVM), is one of several computational methods for solving various problems, including fluid flow. This numerical method is based on the control volume. This concept is applied on a cell level to derive mass, momentum and energy conservation equations from basic laws into a mathematical form known as finite volume equations (FVEs).

Since the transfers are more extreme along the walls and there are discontinuities at the cylinderinlet and exit, it is preferable to discretize the domain using a mesh of variable pitches to eliminate errors and prevent the problems associated with the Runge phenomenon. Therefore, we have chosen the distribution of the nodes obeying the following cosine laws:

$$r(i) = 0.5 * \left\{1 - \cos\left[\frac{\pi*(i-1)}{i_m - 1}\right]\right\} * A \qquad (12)$$

$$z(j) = 0.5 * \left\{1 - \cos\left[\frac{\pi*(j-1)}{j_m - 1}\right]\right\} (13)$$

$$(\delta r)_e = r(i+1) - r(i)\ ;\ (\delta r)_w = r(i-1) - r(i) (14)$$

$$(\delta z)_n = z(j+1) - z(j)\ ;\ (\delta z)_s = z(j-1) - z(j) (15)$$

The field of study is subdivided into a network of finite volumes of dimensions $dv = \Delta r_i * \Delta z_j$ such as$\Delta r_i = 0.5 * [r(i+1) - r(i-1)]; \Delta z_j = 0.5 * [z(i+1) - z(i-1)]$.(16)

Post-Processor (Graphical representation)
The last step of CFD (Figure 1) is called post-processing. Here the results are shown and discussed.

III-1 Dynamic and thermal fields for the configuration B
Figure 5(a,b) shows the radial evolution of the longitudinal dimensionless velocity for different Rayleigh numbers. The influence of the heat source is noted at the system inlet for the two Rayleigh numbers (10^5and10^7). The boundary layer regime (A = 0.3) is characterized by velocity peaks at the axis vicinity and at the system inlet, which is confirmed by experience [8].

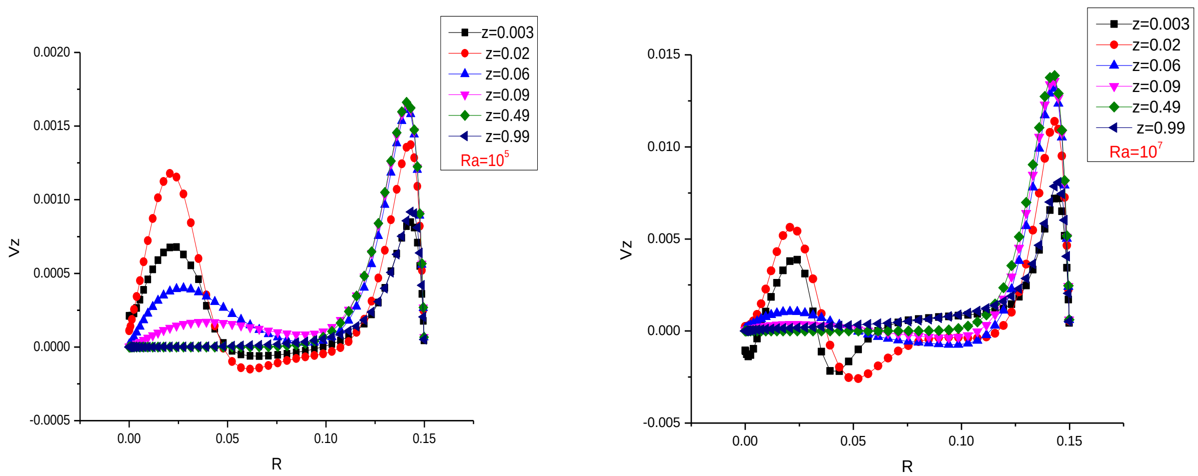

(a) (b)

Figure 5 (a,b):- Radial evolution of the vertical dimensionless velocity at different levels Z of Rayleigh number at (a)$10^5$and(b)10^7.

The influence of the hot source on the air temperature is remarkable at the flow inlet for the form factor (A = 0.3) in **Figure**6.

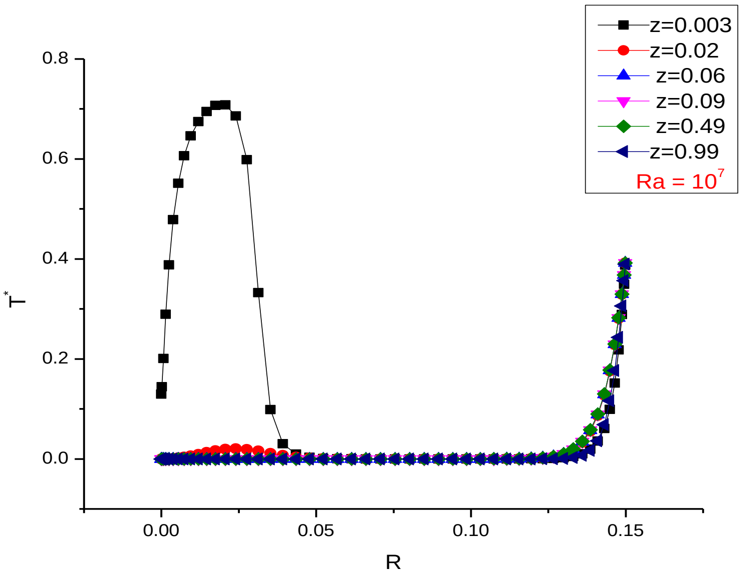

Figure 6:- Radial evolution of the dimensionless temperature at different levels Z of Rayleigh number at 10^7

The axial evolution of the Nusselt number at different values of the Rayleigh number is shown in **Figure7**. An improvement in the heat transfer through the axial direction with the Rayleigh number can be observed.

The Nusselt number characterises the heat transfer by natural convection between the air and the cylindrical wall.

The profiles indicate that the most significant value of convective transfer with walls was obtained at the Rayleigh number 10^{10}. The lowest value was found at the Rayleigh number 10^5.

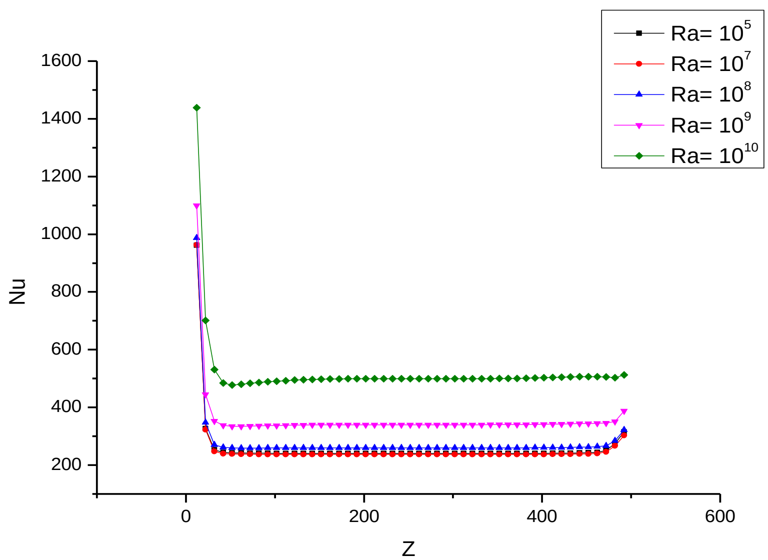

Figure 7:-Axial evolution of Nusselt number at different values of Rayleigh.

The change in the Nusselt number with the Rayleigh number is shown in **Figure8**. This curve follows an exponential variation

Thus, It can be noted that the average Nusselt number increases continuously with the Rayleigh number.

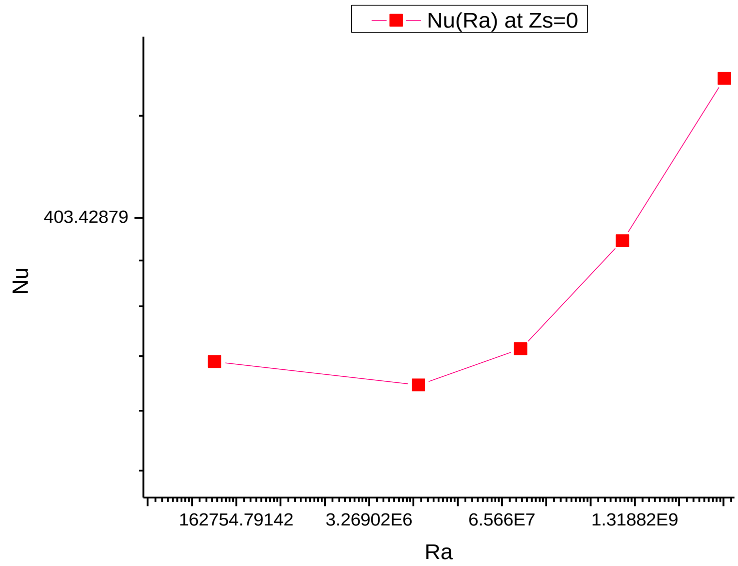

Figure 8:- Influence of Rayleigh number on the Nusselt number.

III-2 Comparison of thermosiphon and thermosiphon with a heating source in velocity and temperature fields
A Comparison of the radial variation of the longitudinal dimensionless velocity is presented in **Figures 9(a, b, c)**. At the cylinder inlet **(Figure 9a)**, the effects of the heat source on the flow are apparent and manifested by a vertical air velocity with two maxima, one near the wall and the other in the vicinity of the hot disc axis. As height increases, the vertical air velocity profile maintains a constant shape and greater intensity **(Figure 9b)**.

Moving the heat source upwards (configuration c) causes a change in the behaviour of the vertical air velocity at the system inlet, as shown in **Figure (9a)**. When the height increases, the vertical velocity profiles are identical in the wall vicinity and differ in the central part at a greater maximum for configuration C in **Figure (9b)**. At the level of the heat source position zs, the vertical velocity is maximum at the axis area, which is explained by the flow supply through this region.

The hot air increases its velocity according to the principle of flow continuity. It appears that the circular shape of the heat source enhances the air mixture and the excellent uniformity of the flow. Therefore, it could be seen that the velocity increases with heat.

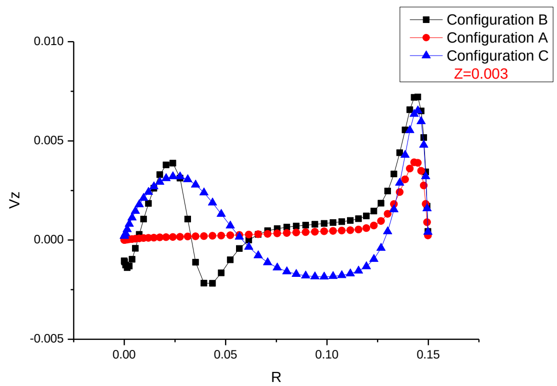

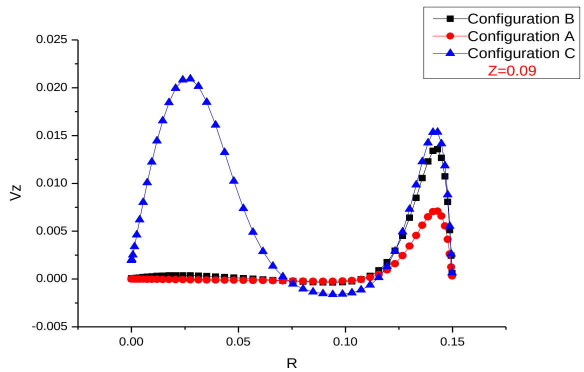

(a) **(b)**

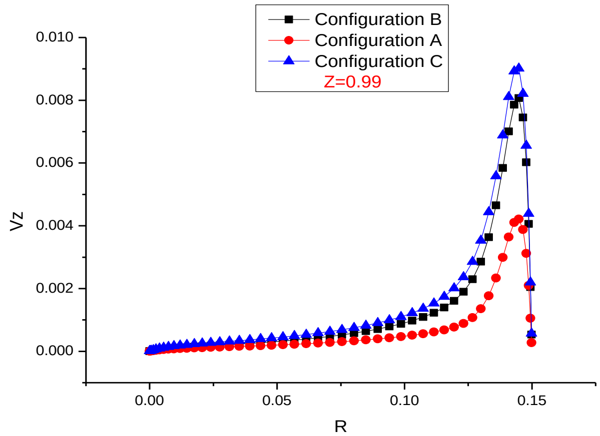

(c)

Figure9(a, b, c):- Comparison of the radial change in the longitudinal dimensionless velocity of the thermosiphon and the thermosiphon with a heating source for the three configurations (a) at the inlet Z = 0.03 (b) at the center Z = 0.09 (c) at the outlet z = 0.99.

A comparison of the radial change in the dimensionless air temperature in the three configurations, A, B and C, is shown in Figure 10 (a and b). The effects of the heat source on the air temperature at the cylinder inlet are reflected by the appearance of a maximum near the hot disc axis **(Figure.10.a)**. As the height increases, the air temperature decreases, and the maximum near the axis flattens considerably, while that near the wall remains elevated **(Figure.10b)**. The profiles show that the air temperature has a maximum at the axis vicinity above the hot disc for configuration B.

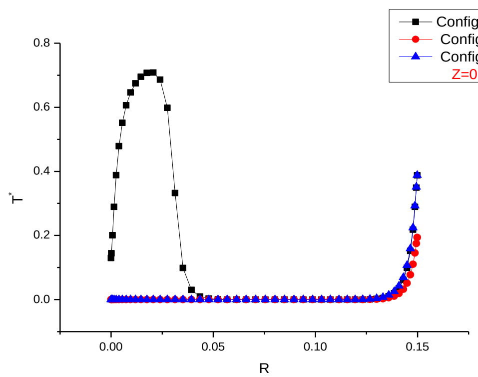

(a)

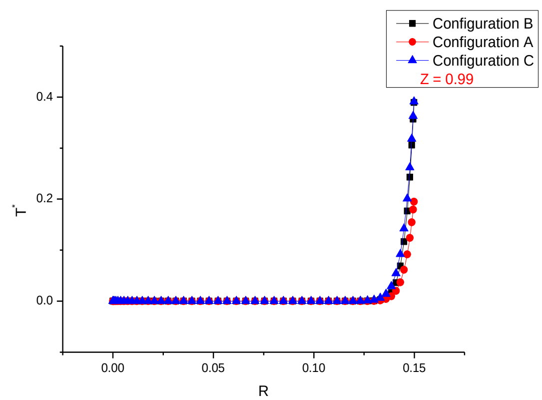

(b)

Figure10:- Comparison of the radial change in the dimensionless temperature of the thermosiphon and the thermosiphon with a heating source for the three configurations (a) at the inlet Z = 0.03 (b) at the outlet z = 0.99.

Comparison of the axial change in Nusselt number for the three configurationsat Rayleigh number 10^7 is shown in **Figure** 10. The local transfer between the wall and the air is more important in configuration B. The profiles revealed that configurations B and C have the highest value of convective transfer with walls, whereas configuration A has the lowest value.

The variation of the Nusselt number with the Rayleigh number is shown in **Figure 11.** A considerable improvement in the Nusselt number is noticed following the introduction of the heat source at the system inlet, showing an increase in the Nusselt number in configurations C and B for low values of the Rayleigh number.

The thermal and flow fields are strongly dependent on the Rayleigh number.

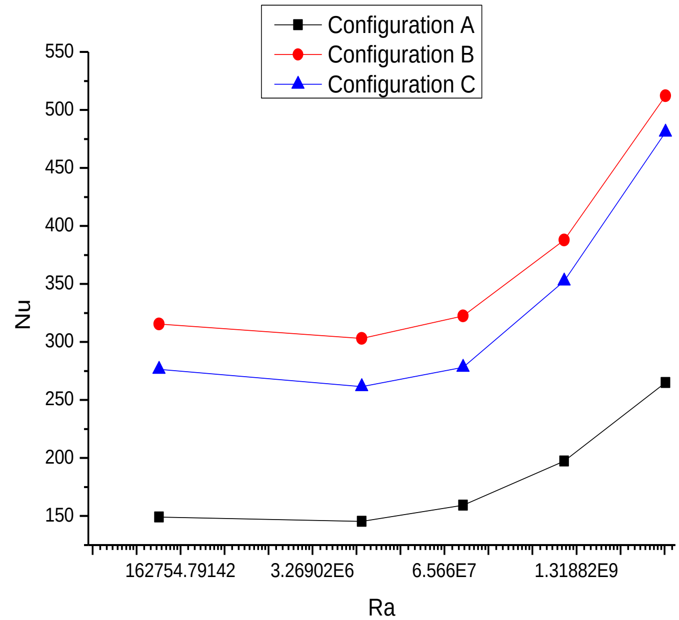

Figure 11:- Comparison of the influence of Rayleigh number on the Nusselt number of the thermosiphon and the thermosiphon with a heating source for the three configurations.

Conclusion:-

In this investigation, the laminar natural convection flow generated in different configurations has been numerically studied using a vertical cylindrical channel and a heat source, based on the Fortran code and using the finite volume method.

The present study investigated two-dimensional laminar flow. The governing equations presented by the Navier–Stokes and energy equations were solved using the finite volume method. The characteristics of the fluid flow inside the cylindrical channel were studied using a different Rayleigh number (Ra = 10^5, 10^7, 10^8, 10^9 , and 10^{10}) and a Prandtl number equal to 0.7 and a form factor A = 0.3 for configurations A, B and, C.

The 501 × 501 mesh exhibits a good compromise between high accuracy and an acceptable computation volume.

Different inlet boundary conditions are used at the cylinder inlet to simulate complex buoyancy-driven natural convection flows. During the investigation, the heat source was changed to a different position at the cylinder inlet (zs = 0 and zs = 0.04).

The results of the study can be summarized as follows:

1- As the heat source is inserted into the cylinder, the effect of the thermosiphon increases and the maxima move towards the wall. In other words, the flow along the radial direction dominates in the lower area of the heat source.

2- In the area near the heat source, we also noticed that the heat source penetration in the cylinder causes speed increase and rapid homogenization of fluid.

3- In laminar flow regimes, the average Nusselt number increases with the increasing Rayleigh number. Therefore, we conclude that they have a direct relationship.

4- Velocity increases with the Rayleigh number and has the same effect on temperature.

5- The presence of the hot disc at different positions improved the heat transfer inside the cylinder.

References:-

[1] T. Naffouti, J. Zinoubi, R. B. Maad, Experimental Characterization of a Free Thermal Plume and in Interaction with its Material Environment. Applied Thermal Engineering, 30, 2010, 1632-1643.
[2] V. I. Terekhov , A. L. Ekaid, The Effect of Aspect Ratio on the Laminar Free Convection inside a Vertical Channel Heated Isothermally. Applied Engineering,2016.
[3] C. F. Kettleborough, Transient Laminar Free Convection between Heated Vertical Plates Including Entrance Effects, International Journal of Heat Mass Transfer, 15,1972, 883-896.
[4] I. Lashgari, F. Picano, W. P. Breugem and L. Brandt, Laminar, Turbulent and Inertial Shear-Thickening Regimes in Channel Flow of Neutrally Buoyant Particle Suspensions. 2014.
[5] A. O. M. Mahmoud, Etude de l'interaction d'un panache thermique à symétrieaxiale avec un écoulement de thermosiphon, Thèse de Doctorat, Université Tunis II, 1998.
[6] B.Jouini, M. Bouterra, A. E. Cafsi and A. Belghith, Numerical Study of the Structure of Thermal Plume in a Vertical Channel: Effect of the Height of Canal. Thermal Science, 20(1), 2016, 67-76.
[7] J.Zinoubi, R. B. Maad, A. Belghith, Influence of the Vertical Source–Cylinder Spacing on the Interaction of a Thermal Plume with a Thermosiphon Flow: An Experimental Study, Experimental Thermal and Fluid Science, 28, 2004, 329–336.
[8]A. M. Mahmoud, Z. Yahya Improvement in the Performance of a Solar Hot Air Generator Using a Circular Cone, 2019.